

# SELECTION AND CONVERSION OF TURBOCHARGER AS TURBO-EXPANDER FOR ORGANIC RANKINE CYCLE (ORC)

Choon Seng Wong<sup>1</sup>, David Meyer<sup>2</sup> and Susan Krumdieck<sup>3</sup>

<sup>1,2,3</sup>Department of Mechanical Engineering, University of Canterbury, Private Bag 4800, Christchurch 8041, New Zealand

<sup>1</sup>[choon.wong@pg.canterbury.ac.nz](mailto:choon.wong@pg.canterbury.ac.nz)

<sup>2</sup>[david.meyer@canterbury.ac.nz](mailto:david.meyer@canterbury.ac.nz)

<sup>3</sup>[susan.krumdieck@canterbury.ac.nz](mailto:susan.krumdieck@canterbury.ac.nz)

**Keywords:** Organic Rankine Cycle, Radial Turbine, Selection of Off-shelves Turbine, Turbocharger, ORC Turbine

## ABSTRACT

The turbo-expander is the most crucial and expensive component in Organic Rankine Cycle (ORC) power generation systems. The turbine engineering, design and research development process for ORC system is costly, time-consuming, and difficult for new-entrants in the ORC field. This paper investigates re-design and retrofit of an off-the-shelf turbocharger for a 1 kW ORC system. The expander requirements were determined for the 1 kW bottoming cycles for Capstone Gas Turbine from the system design. A radial turbine was selected and an off-shelves turbocharger from a small petrol-driven vehicle was acquired. The turbocharger was simulated to study the off-design performance in the ORC system. The turbocharger was evaluated by expansion of compressed air in room temperature to assess the leakage of working fluid and lubrication. A preliminary design was developed to deal with leakage and lubrication issues. The conceptual design of ORC turbine includes the casing design and selection of auxiliary components such as bearings, seals and lubrication system.

## 1. INTRODUCTION

Utilization of low grade heat source for power generation is increasing research and development of ORC systems. The ORC uses refrigerants as working fluids to provide higher thermal cycle efficiency compared to the conventional steam Rankine cycle at resource temperature below 300°C (Vankeirsbilck, Vanslambrouck, Gusev, & De Paepe, 2011). The design and development of turbo-expander for ORC system is the most expensive component in the whole system. Stosic found that turbo-expander in a 1MW ORC system costs over half of the total capital cost (Leibowitz, Smith, & Stosic, 2006). The high cost of the turbo-expander is attributed to the intensive research and engineering development in turbine design and manufacturing process.

The type of turbine has to be selected before proceeding to turbine design and analysis. A wide variety of turbo-expanders can be chosen for ORC applications. Positive displacement machines are popular for small scale ORC systems due to the simplicity and low cost, while turbo-expanders are widely applied for large scale power generation systems and have achieved high turbine efficiency and high reliability. The type of turbo-expander is determined by shaft speed, mass flow rate and the nominal power range. Recent development in small scale ORC systems for research application has produced an expander selection methodology, which covers scroll

expander, screw expander, and radial turbine (Quoilin, Declaye, & Lemort, 2010). Application of scroll expanders is limited to power generation below 30 kW due to the excessive leakage at increasing scroll diameter and scroll height (Quoilin et al., 2010). A screw expander was adopted by ElectraTherm for 100 kW ORC system (Qiu, Liu, & Riffat, 2011). However, the screw expander is not as widely validated as scroll expander and radial turbine. Radial turbines are preferable for a wide range of power generation systems ranging from 10 kW to a few MW. Radial turbines are mass-manufactured and affordable as automotive turbochargers. An ORC system for waste heat recovery application was developed by converting an automotive turbocharger by ABB Schweiz AG (Buerki, Bremer, Paice, & Troendle, 2010).

Radial turbine design for an ORC system has two approaches, turbine design or turbine selection. Turbine design process involves preliminary design of the radial turbine, followed by a computational fluid dynamic (CFD) analysis for the blade design. This approach is typical for turbomachinery developers such as GE Energy and Turboden. However, turbine selection is a more preferable approach for new ORC developers if an existing turbomachine can be retrofitted for ORC. The radial turbine could be developed by retrofitting automotive turbochargers which are easily accessible, relatively low cost, and manufactured in a wide range of sizes. Once a suitable turbine wheel is chosen, auxiliary components have to be selected and the casing has to be re-designed. The turbine selection and retrofit process is shown below.

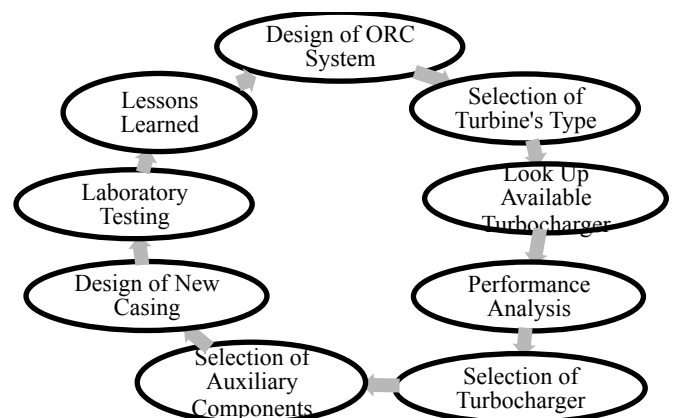


**Figure 1: Selection and Retrofit of a Turbocharger as ORC Turbine**

This paper demonstrates the selection of turbine type, evaluation of performance, and conversion of a turbocharger into an ORC turbine. One-dimensional off-design performance analysis model is coupled with established empirical loss models to estimate the pressure

ratio and isentropic efficiency of the turbine from the turbocharger given inlet thermodynamic conditions. This paper then discusses the required modification in retrofitting the turbocharger as ORC turbine.

## 2. SELECTION OF TURBINE'S TYPE

A number of turbine selection methodologies have been proposed for different types of turbines and expanders for different applications. The selection methodologies were developed by Balje (Balje, 1981), Dixon (Dixon & Hall, 2010), Baines (Japikse & Baines, 1995), and Lemort (Quoilin et al., 2010). Lemort has proposed a selection methodology covering scroll expander, screw expander and radial turbine based on nominal power (Quoilin et al., 2010). Balje, Dixon and Baines have developed turbine classification and selection methodology based on specific speed.

The 1kW ORC system has the system specification as below.

1. Working fluid is R245fa
2. Inlet total temperature,  $T_{01}$  is 370 K
3. Inlet total pressure,  $P_{01}$  is 17 bar
4. Mass flow rate,  $\dot{m}$  is in the range of 0.1 and 0.3 kg/s.

A radial turbine was chosen from turbine performance chart in Figure 2 (Balje, 1981) by assuming specific speed as 0.6. Optimal rotational speed was determined as 59,450rev/min, 42,040rev/min, and 34,320rev/min for 0.1kg/s, 0.2kg/s and 0.3kg/s respectively. An optimal range of specific diameter was determined as 0.28 and 0.38 from Figure 2. By using equation (2), the optimal range of turbine diameter was determined in the range of 9 and 21cm.

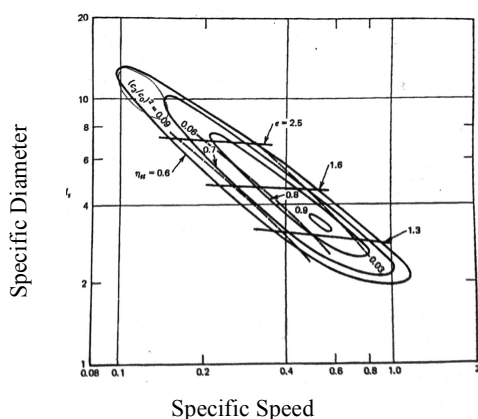


**Figure 2: Performance Chart of Radial Turbine by Balje (Balje, 1981)**

$$n_s = \frac{\omega \sqrt{\dot{m} / \rho}}{(\Delta h_{is})^{0.75}} \quad (1)$$

$$d_s = \frac{D (\Delta h_{is})^{0.25}}{\sqrt{\dot{m} / \rho}} \quad (2)$$

The radial turbine was also chosen for several reasons. The radial turbine is cheaper than axial turbine. The radial turbine is more robust under high blade loading by high density working fluids such as R245fa and stable from the

standpoint of rotor-dynamic due to high stiffness (Ventura, Jacobs, Rowlands, Petrie-Repar, & Sauret, 2012). Table 1 shows geometry and overall dimension of a selected radial turbine (known as TC-1) from a turbocharger for petrol-driven vehicle.

**Table 1: Basic Dimensions Value of Turbocharger TC-1**

	Unit	Value
Inlet radius	$r_1$ (mm)	22.3
Outlet tip radius	$r_{2,tip}$ (mm)	19.3
Outlet hub radius	$r_{2,hub}$ (mm)	6.5
Inlet blade height	$b_{in}$ (mm)	6
Total blade height	$b_{total}$ (mm)	18.5
Blade number	$Z$	9
Inlet blade angle	$\beta_{1,b}$	0
Outlet blade angle at tip	$\beta_{2t,b}$	55
Outlet blade angle at hub	$\beta_{2h,b}$	45

## 3. NUMERICAL MODEL

Off-design performance of radial turbine was first developed in FORTRAN by Glassman as part of NASA gas turbine program since 1970 (Wasserbauer & Glassman, 1975). The performance analysis process was widely applied in performance estimation of turbocharger for both steady-state (Serrano, Arnau, Dolz, Tiseira, & Cervelló, 2008) and unsteady flow condition (Rajoo, Romagnoli, & Martinez-Botas, 2012). The performance model was developed under the assumption of perfect gas, in which ideal gas equation is applied and specific heat capacity is assumed to be constant at all temperature (Meitner & Glassman, 1980, 1983; Wasserbauer & Glassman, 1975). In this study, as the performance analysis was conducted in Engineering Equation Solver (EES), the in-built real gas properties of EES is applied to determine the thermodynamic properties of real fluid instead of using ideal gas law. The fluid behaviour can be predicted at higher accuracy comparing to the application of ideal gas equation. The loss models will not be discussed in detailed as the information can be obtained in the relevant sources.

### 3.1 Passage Loss

Passage loss is defined as total fluid flow loss inside the blade passage, including secondary flow loss, mixing flow loss, the blockage loss, and the kinetic energy loss due to growth of boundary layer along the blade surface (Moustapha, Zelesky, Baines, & Japikse, 2003). Baines's textbook reported that the initial passage loss model by NASA cannot accurately predict the passage loss for all types of radial turbines under different operating conditions. An improved version of passage loss is presented in his work, which is shown below.

$$\xi_{passage} = K_p \left\{ \frac{L_h}{D_h} + 0.68 \left[ 1 - \left( \frac{r_2}{r_1} \right)^2 \right] \frac{\cos(\beta_2)}{b_2/C} \right\} * \left( \frac{W_2^2 + W_1^2}{W_2^2} \right) \quad (3)$$

### 3.2 Incidence Loss

The incidence loss model is developed as a function of change in relative tangential velocity energy of the working fluid (Ghosh, Sahoo, & Sarangi, 2011). The fluid approaches the turbine wheel at an angle different from optimal angle. The optimal relative flow angle is

determined based on the empirical formulation below. The incidence loss is then determined as fluid flow loss at any incidence angle other than the optimal flow angle.

$$\tan(\beta_{1,opt}) = \frac{-1.98 \tan(\alpha_1)}{Z_r \left(1 - \frac{1.98}{Z_r}\right)} \quad (4)$$

$$\xi_{incidence} = \left[ \frac{W_1 \sin(\beta_1 - \beta_{1,opt})}{W_2} \right]^2 \quad (5)$$

### 3.3 Trailing Edge Loss

Trailing edge loss is calculated from the relative total pressure loss (Ventura et al., 2012). The relative total pressure loss is proportional to the relative kinetic energy at the rotor exit (Ghosh et al., 2011). The relative total pressure loss is then converted to enthalpy loss coefficient as below (Ventura et al., 2012).

$$\xi_{ie} = \frac{2}{\gamma M_{2,rel}^2} \frac{\Delta P_{0,rel}}{P_{02,rel}} \quad (6)$$

### 3.4 Tip Clearance Loss

The tip clearance is modelled as an orifice with shear flow inside the passage (Ghosh et al., 2011). A study by Baines shows that radial clearance has strong influence on exit flow condition compared to axial clearance (Moustapha et al., 2003). An in-depth examination has showed that the variations of efficiency with axial and radial clearance are not independent as some cross-couplings exist. The cross coupling coefficient was represented with a coefficient,  $K_{a,r}$  and the tip clearance loss is represented by equation below.

$$\xi_{tip} = \frac{U_1 Z_r}{8\pi} (K_a \varepsilon_a C_a + K_r \varepsilon_r C_r + K_{a,r} \sqrt{(\varepsilon_a \varepsilon_r C_a C_r)}) \quad (7)$$

### 3.5 Windage Loss

Windage loss is frictional loss due to leakage of fluid between the back face of the rotor and the back plate. Daily and Nece (Daily & Nece, 1960) considered a simple case of a disk rotating in an enclosed casing. The empirical equations were modified to account for the frictional torque on the back face of turbine rotor. The loss model was then modified and expressed as power loss (Moustapha et al., 2003) and enthalpy loss (Ghosh et al., 2011). Equation (8) shows the windage loss as enthalpy loss.

$$\xi_{windage} = k_f \frac{\bar{\rho} U_1^3 r_1^2}{2 \pi W_2} \quad (8)$$

### 3.6 Performance Analysis Flow

The performance analysis is conducted by first guess-estimating a value for relative flow velocity at turbine outlet and entropy drop across the turbine wheel. Based on the given turbine dimension, the blade speed is determined. The velocity diagram is then constructed. The thermodynamic properties at both turbine inlet and outlet are then calculated. New value of relative flow velocity is

then calculated from continuity equation. If the error of the relative flow velocity is less than the tolerance value, the calculation process will be iterated to achieve convergence on the relative flow velocity. The individual loss of radial turbine is then calculated from the loss models discussed in previous sections. A new value of entropy drop across the turbine is then calculated. The calculation process will be iterated until convergence is achieved on the entropy drop. Finally, the stage efficiency is calculated based on the calculated loss coefficient. The design process overview is presented in Figure 3.

For rotor with radial blade and no guided nozzle, the relative flow angle  $\beta_1$  is zero and the tangential component of flow velocity  $C_{\theta 1}$  is equal to blade tip speed (Serrano et al., 2008).

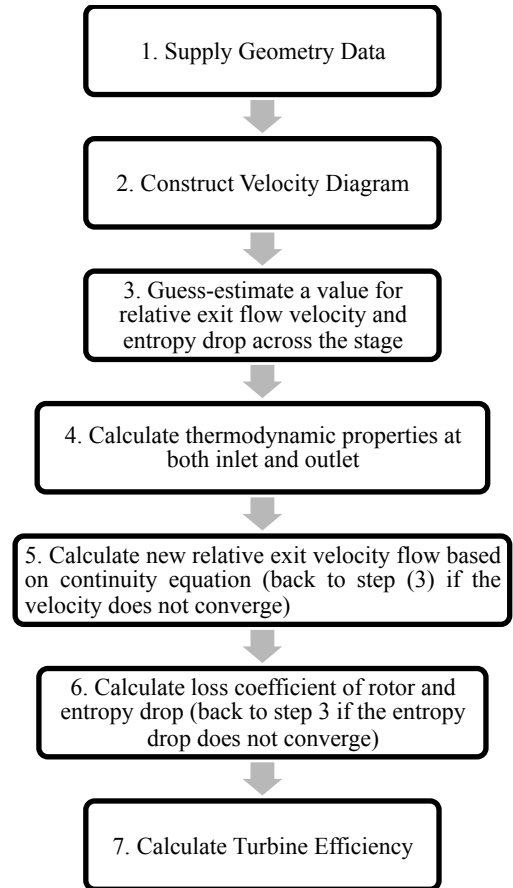


**Figure 3: Performance Analysis of Radial Turbine by Implementing Real Fluid Database**

## 4. PERFORMANCE ANALYSIS OF TC-1

The simulation result shows that the power output of radial turbine is increasing with increasing rotational speed and mass flow rate. From Figure 4, at low rotational speed, the power difference is small for different mass flow rate. However, the power difference is significant for different mass flow rate at high rotational speed. The pressure ratio across the turbine wheel is increasing with rotational speed. At high rotational speed, mass flow rate at 0.1kg/s shows a significant increase in pressure ratio comparing to the pressure ratio by fluid at 0.5kg/s and 1.0kg/s.

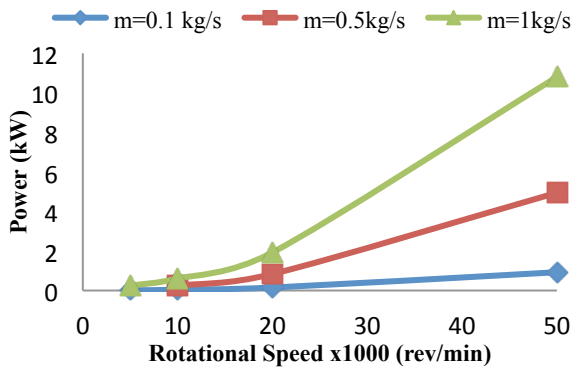


Figure 4: Variation of Power with Shaft Speed and Mass Flow Rate

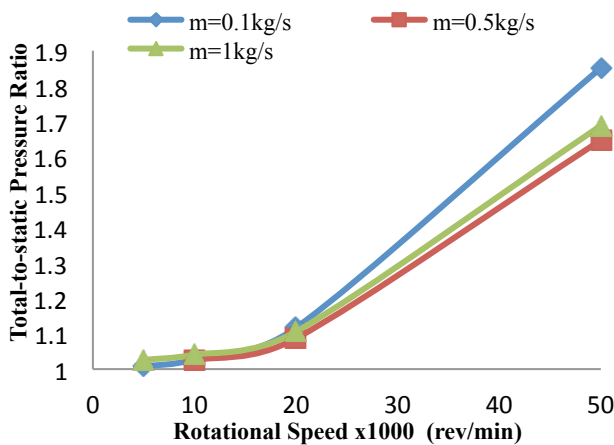


Figure 5: Pressure Ratio across the Turbine Wheel at Different Rotational Speed and Mass Flow Rate

Figure 6 shows the performance curve of different mass flow rate and rotational speed. However, a clear correlation between the investigated parameters is not found. The figure shows an increase in efficiency at 1kg/s up to 20,000 rpm before a constant efficiency between 20,000 and 50,000 rpm. The turbine shows a near-to-constant efficiency at 0.5 kg/s and 0.1 kg/s. However, smaller mass flow rate at 0.1 kg/s shows a lower efficiency (about 55%) compared to the efficiency at 0.5 kg/s (about 77%).

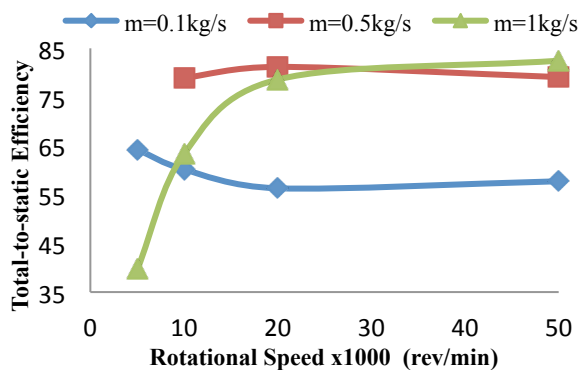


Figure 6: Turbine Total-to-Static Efficiency at Different Rotational Speed and Mass Flow Rate

## 5. EXPERIMENTAL TESTING OF TURBOCHARGER

Turbocharger cannot be directly applied into ORC system due to excessive leakage and poor sealing, unsuitable housing geometry and lubrication issues. The chosen turbocharger was tested in research laboratory in University of Canterbury with the following findings.

### 5.1 Leakages

Excessive leakage was found through the turbo gasket which is sandwiched between the turbine casings. The second major leak site was the bypass valve which is originally used to limit the pressure ratio across the turbine section and prevent over-speed of shaft. The third leak site was along the shaft from the turbine side to the compressor side. Proper seal is not required in turbocharger as the exhaust gas could be safely released to the atmosphere.

### 5.2 Housing Geometry

Turbocharger is usually designed for large exhaust flow rate. Thus, a low pressure ratio was found by testing the turbocharger at small mass flow rate of compressed air at 0.05kg/s. The chosen turbocharger does not have nozzle in directing and accelerating the flow into the turbine wheel thus reducing the overall turbine efficiency. Lastly, the cross-sectional area of the volute is over-sized for the desired mass flow rate. The ORC turbine requires a new design of turbine housing with small inlet flow and inlet nozzle to guide the flow into the turbine wheel.

### 5.3 Lubrication System

Oil-based lubricant is applied to lubricate the bushing and shaft in the turbocharger. The lubrication system is not applicable in the ORC system due to high differential pressure between evaporator outlet and condenser inlet. A separate oil pump with an external oil circuit is required for the ORC turbine. However, the mixture of oil and refrigerant will reduce the lubricating film thickness on the bearing and shaft which will be discussed in the following section. The proposed design would use working R245fa as direct lubrication which is described in the following section.



Figure 7: Laboratory Test Rig of Turbocharger TC-1

## 6. MODIFICATION OF TURBOCHARGER INTO ORC TURBINE

This section discusses the modification required to convert a turbocharger into ORC turbine. From the laboratory testing of the turbocharger, it was concluded that the turbine wheel would be adapted but the casing and bearing would be re-designed and re-selected. The turbine casing would be re-designed with fully enclosed model to avoid leakage through open drive shaft. The turbine shaft would be coupled with a magnetic coupling which facilitates the coupling with an external high speed generator. O-ring would be installed between the turbine casings to prevent leakage of high pressure working fluid through the casing's gap. Figure 8 and Figure 9 show the proposed design of ORC turbine by retrofitting the turbocharger. Modular block design is proposed in the design of prototype due to simplicity in manufacturing process.

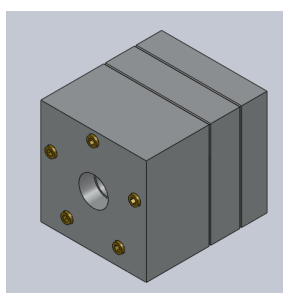


Figure 8: Isometric View of Proposed ORC Turbine

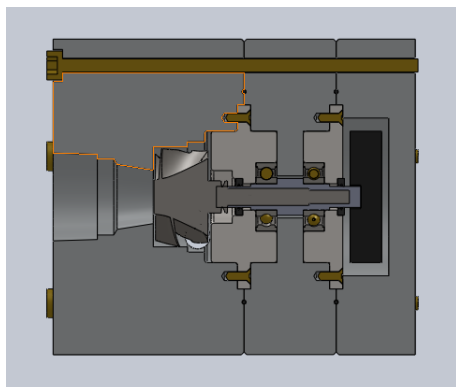


Figure 9: Proposed Design of ORC Turbine by Retrofitting a Turbocharger

### 6.1 Selection of Bearing

Bearings are required to support a rotor shaft in the turbine assembly. The turbine assembly commonly requires radial bearings and thrust bearings to support both the radial load and axial thrust. Literature reviews on steel bearing and hybrid bearing show that hybrid bearing is the most suitable bearing for ORC application.

In a study by Molyneaux, hybrid bearing was found to be more suitable as ORC bearing compared to steel bearing (Molyneaux & Zanelli, 1996). The application of hybrid bearing for refrigerant has also been suggested by Jacobson as hybrid bearing shows an optimization of raceway topography to ensure a maximum elastic deformation of the asperities in the Hertzian contact compared to steel bearing (Jacobson & Espejel, 2006). The optimization of the raceway allows an effective separation of the mating

surfaces, further allows the bearing to withstand pure refrigerant lubrication at long period (Jacobson & Espejel, 2006). The proposed design of ORC turbine would be equipped with hybrid bearing to allow longer life cycle under lubrication of the pure refrigerants.

### 6.2 Selection of Lubricants

In an ORC application, bearings are usually lubricated by the working fluid for small size turbo-generator while bearings for medium size turbo-generator are lubricated by proper oil lubricants with a separate oil circuit and oil pump. Two journal bearings and a thrust bearing are lubricated with R134a in an 18 kW oil-free compressors investigated by Molyneaux (Molyneaux & Zanelli, 1996) and journal bearing and thrust bearing are lubricated with toluene in a 25 kW solar-powered ORC system investigated by Nesmith (Nesmith, 1985). Common issues in bearing failures by using refrigerants include the attack of bearing surfaces by some refrigerants such as ammonia (Jacobson & Espejel, 2006). Many refrigerants tend to dissolve into lubricants, such as R134a in ester oil. The mixture reduces the initial lubricant viscosity and pressure viscosity coefficient thus reducing the film thickness during operations. Furthermore, the boiling point of refrigerant-oil mixture is reduced at the local pressure (Yamamoto, Gondo, & Kim, 2001). The reduction in boiling point allows vaporization of lubricant on the bearing surface when the bearing surface temperature is higher than the boiling point of the mixture, thus reducing the lubricant film thickness (Jacobson & Espejel, 2006). Due to the high cost and complexity of the external lubrication system, the ORC turbine would use the working fluid as lubricant for the bearings.

SKF studies rheology of three working fluids, R245fa, R134a and R123 to choose an optimal lubricant for bearing. Among the three working fluids, R245fa is found to be a better lubricant for rolling bearings followed by R134a and lastly R123. Though R134a is a relatively poor lubricant compared to R245fa, R134a is employed as lubricant for oil-free compressor (Molyneaux & Zanelli, 1996) as the pressure viscosity coefficient of R134a is very similar to the pressure viscosity coefficient of poly alpha olefin oil (Jacobson & Espejel, 2006). The proposed design of turbo-expander in Figure 9 is designed to be lubricated by R134a and R245fa.

### 6.3 Casing Design and Seal Selection

The turbine casing can be categorized into fully enclosed design and open-drive design. In an open drive design, the turbine shaft is coupled to an external generator for power generation. The working fluid will leak to atmosphere due to high differential pressure between the fluid inside the turbine and the atmosphere. The most common sealing system for open drive system is dry gas seal and mechanical seal which are not suitable for small size turbo-generator. The need of an extra gas buffer system and lubrication system to the seal has increased the cost of the turbo-generator.

In a fully enclosed design, the turbine shaft is coupled to a high speed generator within the enclosed casing. However, due to the scarcity of off-the-shelves high speed generator, the proposed design of ORC turbine is connected to magnetic coupling which facilitates the coupling to an external generator. The casing surrounding the magnetic

coupling is made from aluminium to allow the operation of magnetic coupling.

## 6. CONCLUSION

This paper presents the selection of turbine type, performance evaluation of the automotive turbocharger and modification of the turbocharger into an ORC turbine. A suitable type of turbo-expander was chosen from Balje's turbine performance chart. Performance analysis was then conducted to study the performance behaviour of the chosen turbocharger. If two or more turbochargers are chosen during the selection stage, simulation of turbine off-design performance can assist the selection of the turbine wheel. Lastly, this paper demonstrates the conceptual design stage of ORC turbine considering casing design and the selection of bearing, lubricants and seals.

## 7. FUTURE WORK

The future work is categorized into two parts, which are improvement of turbine wheel performance and construction of ORC turbine. The first section revolves around the performance improvement of the turbine wheel. There are two ways to improve the performance of an existing turbine, which are trimming of turbine wheel and inclusion of nozzle. Both methods will be evaluated by using one-dimensional performance analysis methods to compare the performance improvement. Computational fluid dynamic (CFD) analysis will then be conducted to study the optimal blade profile after trimming to achieve optimal efficiency.

The second section aims to construct a prototype of the ORC turbine. Laboratory performance testing and rotor-dynamic balancing will then be included.

## ACKNOWLEDGEMENTS

This work was supported by the New Zealand Heavy Engineering Research Association funded by Ministry for Science & Innovation contract. The authors would like to thank ORC research team in University of Canterbury in helpful feedback in the turbocharger modification and conceptual design process. The authors would like to specially acknowledge Ariff Ghazali from ORC Final Year Project team in assisting the construction of turbocharger test rig and the laboratory testing of turbocharger.

## REFERENCES

- Balje, O. E. (1981). *Turbomachines: A Guide to Design Selection and Theory*: Wiley.
- Buerki, T., Bremer, J., Paice, A. D., & Troendle, D. (2010). Use of a Turbocharger and Waste Heat Conversion System: EP Patent 2,092,165.
- Daily, J., & Nece, R. (1960). Chamber dimension effects on induced flow and frictional resistance of enclosed rotating disks. *Journal of Basic Engineering*, 82, 217.
- Dixon, S. L., & Hall, C. (2010). Fluid Mechanics and Thermodynamics of Turbomachinery Retrieved from <http://canterbury.eblib.com.au/patron/FullRecord.aspx?p=534952>
- Ghosh, S. K., Sahoo, R., & Sarangi, S. K. (2011). Mathematical Analysis for Off-Design Performance of Cryogenic Turboexpander. *Journal of fluids engineering*, 133(3).
- Jacobson, B. O., & Espejel, G. E. M. (2006). High Pressure Investigation of Refrigerants HFC245fa, R134a and R123.
- Japikse, D., & Baines, N. C. (1995). *Introduction to turbomachinery*: Concepts ETI.
- Leibowitz, H., Smith, I. K., & Stosic, N. (2006). Cost Effective Small Scale ORC Systems for Power Recovery From Low Grade Heat Sources. *ASME Conference Proceedings*, 2006(47640), 521-527.
- Meitner, P. L., & Glassman, A. J. (1980). Off-Design Performance Loss Model for Radial Turbines with Pivoting, Variable-Area Stators: DTIC Document.
- Meitner, P. L., & Glassman, A. J. (1983). Computer Code for Off-Design Performance Analysis of Radial-Inflow Turbines with Rotor Blade Sweep: DTIC Document.
- Molyneaux, A., & Zanelli, R. (1996). Externally pressurised and hybrid bearings lubricated with R134a for oil-free compressors.
- Moustapha, H., Zelesky, M., Baines, N. C., & Japikse, D. (2003). *Axial and Radial Turbines*: Concepts ETI.
- Nesmith, B. (1985). Bearing development program for a 25-kWe solar-powered organic Rankine-cycle engine: Jet Propulsion Lab., Pasadena, CA (USA).
- Qiu, G., Liu, H., & Riffat, S. (2011). Expanders for micro-CHP systems with organic Rankine cycle. *Applied Thermal Engineering*, 31(16), 3301-3307. doi: 10.1016/j.applthermaleng.2011.06.008
- Quoilin, S., Declaye, S., & Lemort, V. (2010). Expansion Machine and fluid selection for the Organic Rankine Cycle.
- Rajoo, S., Romagnoli, A., & Martinez-Botas, R. F. (2012). Unsteady performance analysis of a twin-entry variable geometry turbocharger turbine. *Energy*, 38(1), 176-189.
- Serrano, J., Arnau, F., Dolz, V., Tiseira, A., & Cervelló, C. (2008). A model of turbocharger radial turbines appropriate to be used in zero-and one-dimensional gas dynamics codes for internal combustion engines modelling. *Energy Conversion and Management*, 49(12), 3729-3745.
- Vankeirsbilck, I., Vanslambrouck, B., Gusev, S., & De Paepe, M. (2011). Organic rankine cycle as efficient alternative to steam cycle for small scale power generation. *Proceedings of 8 th International Conference on Heat Transfer, Fluid Mechanics and Thermodynamics, Pointe Aux Piments (Mauritius)*.
- Ventura, C., Jacobs, P. A., Rowlands, A. S., Petrie-Repar, P., & Sauret, E. (2012). Preliminary Design and Performance Estimation of Radial Inflow Turbines: An Automated Approach. *Journal of Fluids Engineering-Transactions of the Asme*, 134(3).
- Wasserbauer, C. A., & Glassman, A. J. (1975). FORTRAN program for predicting off-design performance of radial-inflow turbines. *NASA Technical Paper(TN D-8063)*.
- Yamamoto, Y., Gondo, S., & Kim, J. (2001). Solubility of HFC134a in Lubricants and Its Influence on

Tribological Performance. *Tribology transactions*,  
44(2), 209-214.

#### **NOMENCLATURE**

*C*: chord length (m); *D*: diameter (m); *L*: length (m); *M*: Mach number; *m*: mass flow rate (kg/s); *K*: coefficient; *P*: pressure (kPa); *r*: radius (m); *T*: temperature (K); *U*: turbine blade speed (m/s); *W*: relative flow velocity (m/s); *Z*: blade number;

#### *Greek symbols*

$\alpha$ : absolute flow angle;  $\beta$ : relative flow angle;  $\varepsilon$ : clearance;  
 $\xi$ : turbine loss coefficient;  $\rho$ : density;  $\gamma$ : specific heat ratio

#### *Subscripts*

*0*: Stagnation condition; *1*: turbine inlet; *2*: turbine outlet; *a*: axial; *b*: blade; *h*: hydraulic; *opt*: optimal; *p*: passage; *r*: rotor or radial; *rel*: relative; *te*: trailing edge